Flame Characteristics of a Rotating Pool Fire

Sugawa O.[1], Kamiya K.[1,]*, Watanabe N.[2]

[1] *Suwa University of Science, Department of Mechanical Engineering, Chino-shi, Nagano pref., Japan*
[2] *Suwa University of Science, Graduate School of Engineering and Management, Chino-shi, Nagano pref., Japan*
**Corresponding author's email: sugawa@rs.sus.ac.jp*

ABSTRACT

Tangential air flow can generate a fire whirl characterized by unique flame shapes that extend upwards. In this work, the temperature profiles along the centre axes of fire whirl flames were obtained using a series of thermocouples. A circular fire source and a varying number of polycarbonate guide plates were set on a turntable, which was rotated clockwise or anticlockwise. The rotation rate ranged from -90 (anticlockwise) to +150 rpm (clockwise). In trials without guide plates, the flame height increased along with the rotation rate except for slow rotation in the range of 0 to +30 rpm, during which precessional movements were observed. With guide plates, the heat release rate increased with increases in the rotation from 0 to -90 rpm, and the data strongly suggest that the heat release rate was proportional to the degree of air circulation. Over the rotation range of -60 to -70 rpm and with guide plates the fire whirl changed from a slender flame shape to a thick tubular morphology having an eye wall. The excess temperatures, ΔT, along the centre axis of a flame produced with guide plates indicated the absence of an intermittent flame region, which is typically observed in free burning flames. The behaviour of this flame was therefore significantly different from that of a general pool fire.

KEYWORDS: Fire whirl, tubular fire whirl, rotation tube, heat release rate.

NOMENCLATURE

D	pool diameter (m)
H	flame height (m)
M	fuel mass (g)
Q	heat release rate (kW)
R	pool radius (m)
Γ	ambient circulation (m^2/s)

Subscripts

*	dimensionless

INTRODUCTION

In contrast to a free buoyant fire, fire whirls can generate unusual, swirling diffusion flames with increased combustion rates relative to those in a free burning pool fire. In addition, the upward flame extension can be several times the diameter of the combustion zone and the flames can emit significant heat radiation that is damaging to surrounding materials. Fire whirls have been observed during both unconfined vegetation and residential fires, and are characterized by tall, slender or conical swirling flames with diminished flame tops [1]. A typical fire whirl is shown in Fig. 1(a). An extreme fire whirl that assumed a tubular shape was observed in 1923 in the Honjo district of Tokyo, Japan, in the aftermath of the Great Kanto earthquake, and was captured in a well-known painting, as shown in Fig. 1(b) [2]. In this case, the flame shape was quite different from a typical fire whirl morphology and had a thick, tubular, swirling appearance. This tubular fire whirl caused

Proceedings of the Ninth International Seminar on Fire and Explosion Hazards (ISFEH9), pp. 642-651
Edited by Snegirev A., Liu N.A., Tamanini F., Bradley D., Molkov V., and Chaumeix N.
Published by St. Petersburg Polytechnic University Press
ISBN: 978-5-7422-6496-5 DOI: 10.18720/spbpu/2/k19-58

significant loss of life and property damage in Tokyo [3-5]. Most available literature regarding fire whirls is focused on the quasi-steady behaviour of a slender or conical swirling flame and a small number of papers [6-7] address tubular flames. Data regarding such fire whirls having free boundaries are very limited, even though tubular burners, in which a rotating flame is generated inside a cylinder, are often employed in industrial applications for heating purposes due to their high efficiency [8-9].

Many experimental studies [6-7, 10-16] of fire whirls having the typical tall, slender or conical flame shape have been carried out, using either guide plates or circulation cage facilities. Guide plates, or slides consisting of a pair of half tubes, induce a circular air flow in the flame zone based on tangential entrainment resulting from the buoyant force of the flame and the ingress of air through gaps in the guide plates or half tubes. In contrast, a tubular cage apparatus employs a mechanically-rotated screen to produce a fire whirl from a flame inside the cage [7]. Snegirev et al. [6] made tubular whirling flames using the chimney effect in a chamber and simulated numerically its behaviour based on the observations. The present experimental study attempted to produce a tubular fire whirl using the guide plates method with the aim of developing an approach to reproduce the tubular fire whirl at a small laboratory scale, as well as to get further understanding on the behaviour of tubular fire whirls.

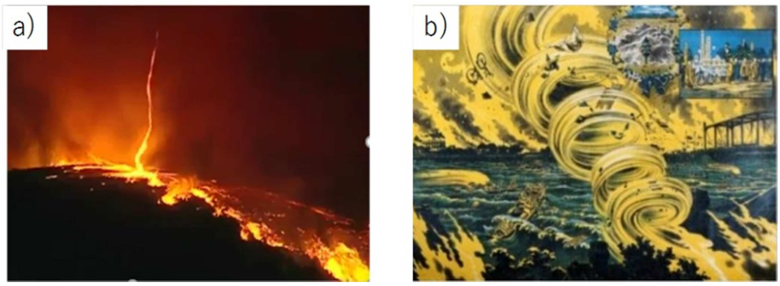

Fig. 1. a) A photographic image of a typical fire whirl [1] and b) a historical painting of a tubular fire whirl [2].

EXPERIMENTAL

Experimental apparatus

To either avoid or shorten the flame precession period in preliminary assessments of the fire whirl, tests were carried out using 12, 14 or 16 guide plates without rotation prior to the main trials. These tests indicated that a longer time span was required to progress from the precession flame mode to the formation of a straight upwards fire whirl when employing 12 or 14 plates compared with 16 plates. The fire whirl generated with 16 guide plates was also found to be more stable, and so this number of plates was adopted for use in the main tests. Two different types of experimental apparatus were employed. One comprised a rotating table surrounded with a wire screen while the other consisted of a rotating table surrounded by guide plates. Both systems were set inside a larger cylindrical mesh screen to prevent any interactions with the laboratory ventilation system. Figure 2 presents diagrams of the experimental apparatus, consisting of a turntable and polycarbonate boards with dimensions of 55 mm (width) × 500 mm (length) × 4 mm (thickness) arranged around the circumference of the table. A set of 16 guide plates was arranged around a 140 mm radius circumference to form an almost regular hexadecagonal fixed cage. These guide plates were inclined against the circumference by 10°, with gaps between the plates.

A cylindrical porcelain vessel with an inner diameter of 54.4 mm and a height of 23.4 mm was set at the center of the turntable and served as the flame source. The liquid fuel in all trials was 2-propanol and this fuel was supplied to the vessel through a tube before each test, after which the exact fuel mass was measured by an electric balance. The vessel was warmed by burning a quantity of fuel prior to each trial, so that the initial temperature of the vessel was almost constant at approximately 80°C (close to the boiling point of the fuel).

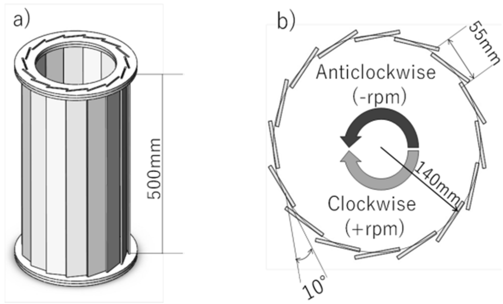

Fig. 2. Diagrams of the experimental apparatus, showing a) the exterior with guide plates and b) an overhead view of the guide plates arrangement and rotation directions.

Measurement technique

The turntable was placed on a Mega-Torque motor (M-YS2020FN001, NSK) that permitted stable, controlled clockwise or anticlockwise rotation. In the first series of tests, the fire source was set at the center of the table without guide plates so as to observe the flame shape, and only clockwise rotation (0 to 150 rpm) was employed because there was no entrainment mechanism induced by axisymmetric rotation without the guide plates. In the second series of tests, 16 guide plates were placed around the circumference; they were set without rotation to establish the shape of the fire whirl and to determine the shortest precession time-period.

In the third series of tests, both the fire source and the 16 guide plates were employed, and they were rotated either clockwise or anticlockwise via the turntable, as shown in Fig. 2(b). Herein, clockwise rotation is represented by a "+", while anticlockwise is denoted by a "-" sign. The rotation rate ranged from -90 to +90 rpm.

Several digital video cameras (HDR-CX535 and HDR-AS200V, SONY) were positioned above and beside the flame to record the flame shapes. The temperatures along the central axis of the fire whirl were measured using type K thermocouples (0.32 mm diameter) at 12 locations from the upper part of the fire source to the highest point of the tubular cage. These positions were at heights of 0, 0.05, 0.07 (or 0.1), 0.14 (or 0.19), 0.21 (or 0.28) and 0.64 m above the source. The output signals from the thermocouples were recorded using a data logger (NR-600, KEYENCE) at 1 s intervals. The temperature values were determined during steady-state combustion and processed to obtain the time-averaged temperatures. The average fuel combustion rate, which reflects the average heat release rate (HRR), was estimated based on the mass of fuel consumed from ignition to extinction. Flame heights were determined from images captured by the cameras, using 180 consecutive frames during the stationary combustion state to determine time-averaged heights. As noted, all experiments were performed using a screen surrounding the cage and turntable to avoid any effect of the laboratory ventilation system.

RESULTS

Heat release rate with rotation

Figure 3 shows the relationship between the HRR and the rotation rate for tests carried out without guide plates. The data for a trial with neither rotation nor plates indicate an average HRR of 1.04 kW, and the same test without guide plates but with rotation from 0 to 10 rpm gave almost the same

HRR values (in the range of 1.04 to 1.05 kW). Thus, rotation in this range did not result in a significant extension of the flame height. In trials without the guide plates, the HRR increased in an almost linear manner with increases in the rotation rate. The maximum HRR of 2.47 kW at 150 rpm was almost 2.5 times greater than that obtained without rotation. The increased rotation rates served to increase the degree of flame whirling as well as to promote the accompanying air flow. These factors enhanced the HRR and extended the flame height whether the rotation direction was clockwise or anticlockwise. The plots of HRR as a function of rotation rate demonstrate that the circulation rate of the fire whirl was proportional to the HRR.

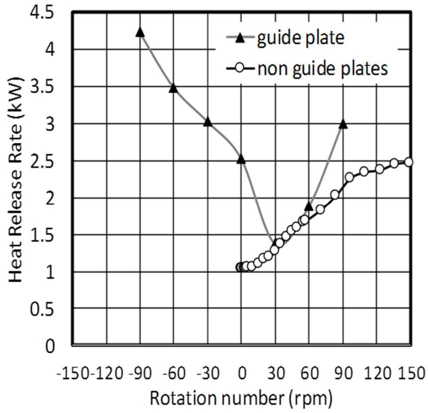

Fig. 3. Relationship between rotation rate and heat release rate.

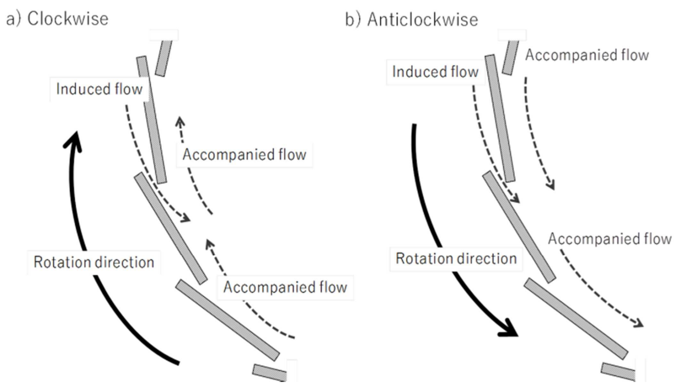

Fig. 4. Diagrams showing changes in the induced air flow and accompanied flow with variations in the rotation direction.

The buoyant vertical current in the tube promoted air flow from the exterior of the tube into the internal space and this air entered tangentially through the gaps between the guide plates. The tangential air provided a rotational driving force to the flame even at 0 rpm (that is, no rotation). The tangential gaps between the guide plates also served to draw air into the tube during clockwise rotation, as shown in Fig. 4(a). Subsequently, the accompanied air flow driven by the walls and guide plates encountered the thermally-induced air flow. These two flows (the accompanied that was clockwise and the induced that was anticlockwise) met, leading to stagnation around the upward flame. Thus the flame showed precession or meandering movements and little extension upward. The use of 16 guide plates with a 10° tangential inclination resulted in stagnation of the air flow around the flame due to competition between clockwise and anticlockwise flow at a rotation rate of +30 rpm. Stagnation also appeared in the range of 0 to +30 rpm, and the precession and/or meandering movement of the flame was found to reduce both the HRR and the flame height, as shown in Fig. 4(a). This meandering flame motion continued up to a rotation rate of approximately +60 rpm.

At higher rates of rotation, the motion transitioned to an almost straight rotating movement together with whirling and upwards extension of the flame. This occurred because the increased clockwise rotation was sufficient to overcome the stagnation effect and drive the flame into a whirling mode. Interestingly, imparting an anticlockwise rotation (Fig. 4(b)) did not produce a meandering flame movement, resulting in a much higher HRR. The volume of entrained air was increased as the anticlockwise rotation rate was increased, which would be expected to promote combustion. Clockwise rotation of +90 rpm gave HRR of 3kW, which corresponded to the same HRR for an anticlockwise rotation of -30 rpm. If the anticlockwise rotation interrupted to the corresponded clockwise rotation based on HRR values, anticlockwise rotation corresponded to +90 to +180 rpm including no rotation. It is believed that rotation of the tube entrained surrounding air into the flame, resulting in increased HRR as the rotation rate was raised as shown in Fig. 5.

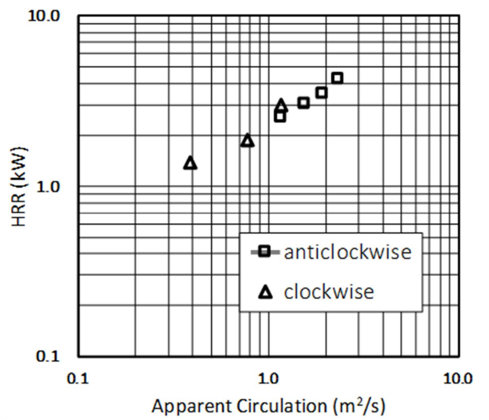

Fig. 5. Heat release rate versus apparent circulation.

Flame height as a function of rotation rate

Figure 6 presents photographic images of representative flame shapes and behaviours. Figure 6(a) shows the flames obtained without guide plates, and indicates that the flame height increased with increases in the rotation rate; however the flame height approached a plateau as the flame changed to tubular shape. The flames exhibited precession in the initial stage of every experiment and rarely stood upright. Rather, the tips of the flames swayed in various directions. Figure 6(b-1), which presents images of the flames that were observed in the tests carried out with guide plates, indicates that the flame heights obtained at 0 and +90 rpm with clockwise rotation were at almost the same level. However, the flame heights at rates from +30 to +60 rpm were lower than those at 0 rpm because the flame underwent precession. Figure 6(b-2) shows that, during rotation from -30 to -90 rpm, precession was not evident and the flame heights were essentially almost equal to that at 0 rpm. Even so, the widths of the flames increased with anticlockwise rotation rates. Figure 6(d) provides overhead images of flames obtained with the use of guide plates over the rotation range from 0 to -90 rpm. The bright portion of each photograph shows the flame region. The bright flames in the center of these images appear at rotation rates from 0 to -60 rpm, and have almost equivalent heights, as were observed by Lei et al. [7]. At rates of -60 to -70 rpm, the center part of the flames darkened and the flames acquired tubular or hollow shapes. This tubular flame shape continued up to a rate of -90 rpm (Fig. 6(d)). These whirling, tubular flames had very different shapes from those of typical fire whirls, which tend to be slender, long and meandering, but were similar to the tubular whirling flame observed following the Kanto earthquake.

Figure 7 plots the relationship between the clockwise and anticlockwise rotation rates and the experimental flame height (H) ratioed to the flame height (H_0) obtained during free burning (without guide plates or rotation). Without guide plates, the flame height was increased at rates of

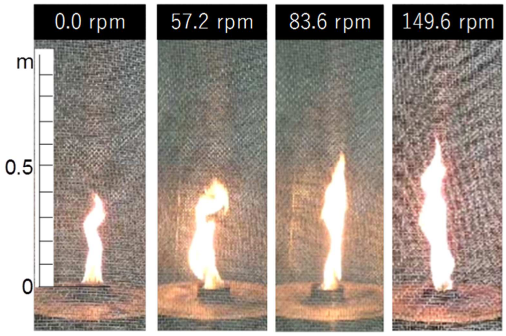

□) R□t□ti□□with□□t g□id□pl□t□s (sid□vi□w)

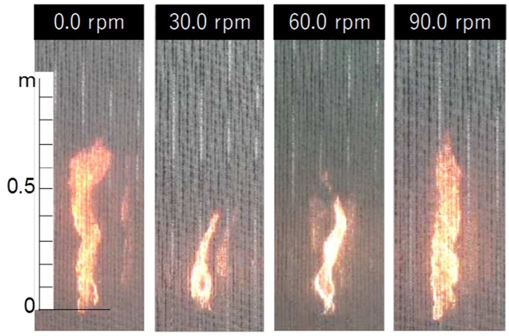

b-1) With g□id□pl□t□s (sid□vi□w)

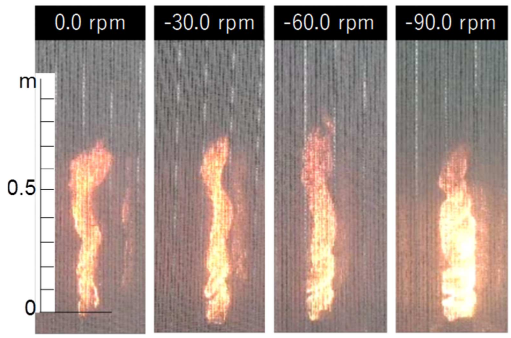

b-2) With g□id□pl□t□s (sid□vi□w)

□) With g□id□pl□t□s □s □□pt□□□d by high sp□□d □□m□□□(-60 □pm)

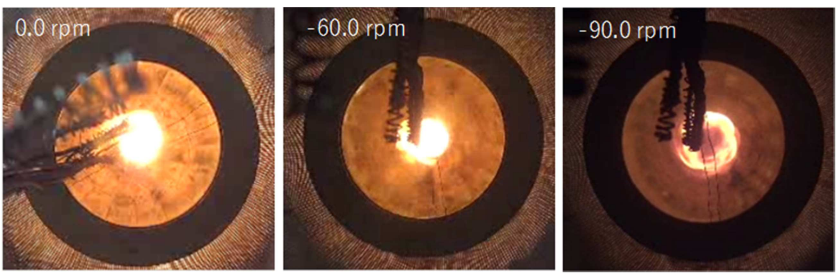

d) With g□id□pl□t□s (t□p vi□w)

Fig. 6. □h□t□g□□phi□im□g□s □f fl□m□sh□p□s □□d b□h□vi□□s. Th□im□g□i□(□) w□s □□q□i□□d □si□g □high-sp□□d □□m□□□□d sh□ws □fi□□whi□l m□□h lik□th□t i□Fig. 1(b).

+60 rpm or higher and plateaued between +120 and +150 rpm. The test carried out without rotation (0 rpm) but with guide plates resulted in flame extension to a height 1.8 times that observed during free burning. It appears that air entrainment through the gaps produced a slender flame due to rotation and the accompanying tangential air flow. Upon changing the rotation from anticlockwise to clockwise, the flame height ratio began to decrease at approximately 0 rpm and approached a value of 1 at approximately +30 rpm. As shown in Fig. 6, the trials with guide plates showed a decrease in the flame height ratio with the anticlockwise rotation rate. At the same time, the flame shape became less slender and stood almost straight, while adopting a precessional movement. However, the flame height ratio increased once again after stagnation was induced at +90 rpm. Using an anticlockwise rotation resulted in no major changes in the flame height ratio upon increasing the rotation rate. This manner was similar to those observed by Lei et al. [7]. The H/H_0 value remained steady at approximately 2. In these trials, the correlation between the flame height ratio and the rotation rate was equivalent to that between the HRR and the rotation rate in Fig. 3, regardless of the presence of guide plates. These flame shape changes (from slender to tubular fire whirl) in increased rotation were similar to those presented in the flame pattern diagram by Lei et al. [7]. Based on the present experiments, the slender flame changed to tubular flame at around the condition which had Γ of 1.93 (m^2/s) at HRR of 3.49 kW, and a tubular fire whirl was clearly established for Γ of 2.32 (m^2/s) at HRR of 4.23 kW after the transition in flame shape. These flames corresponded with the flame of "cylindrical fire whirl" in the pattern map of Q-Γ [7], indicating the good guidance and categorized regions of flame shapes with whirling.

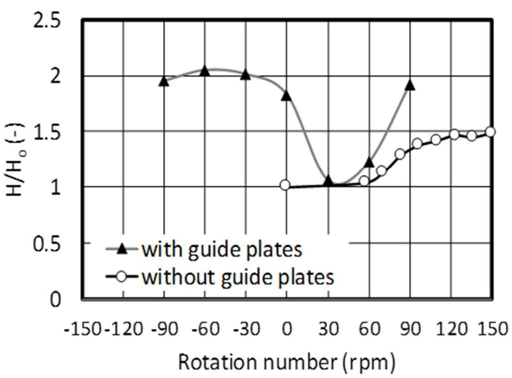

Fig. 7. The relationship between rotation rate and flame height ratioed to the height during free burning (that is, without guide plates or rotation).

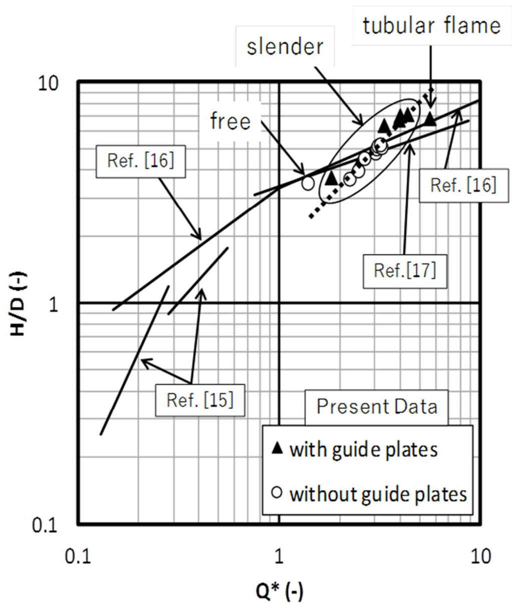

Fig. 8. The relationship between the flame height and the non-dimensional heat release rate, based on data from Cox and Chitty [18], Zukoski [19] and Thomas [20].

The flame height for a typical pool fire can be correlated with HRR (Q) or with the non-dimensional heat release rate (Q*) based on the Froude model. This model takes into account the balance between buoyancy and the inertial force when considering combustion within the flame. In the case of a fire whirl, air circulation (Γ) increases both the height and apparent diameter of the flame. If Γ is circulation, representing the balance between centripetal and centrifugal force in the flame, we can write $H/D \sim (Q^{*\alpha}\ \Gamma^{*\beta})$, where the coefficients α and β have to be determined experimentally. Wang et al. [17] showed that the non-dimensional flame height (H/D) can be correlated with these terms according to $H/D \sim (Q^*\ \Gamma^{*2})^{0.33}$. This same group also determined that the mass loss rate (m/R) is correlated with the non-dimensional circulation (Γ^*) according to $(m/R) \sim \Gamma^{*1.08}$. These correlations can be rewritten in more general terms as

$$H/D \sim (Q^*\ \Gamma^{*2})^{1/3}$$

and

$(m/R) \sim \Gamma^*$,

while keeping their physical meanings. It can also be assumed that the mass loss rate equals the heat release rate. As such, the non-dimensional flame height (*H/D*) will be proportional to the non-dimensional heat release rate, so that $(m/R) \sim (Q^*)$ can be written, and $(Q^*) \sim \Gamma^*$. Based on these relationships, Γ^* in $(Q^*\Gamma^{*2})$ can be replaced by (Q^{*3}). Thus, $H/D \sim (Q^* \Gamma^{*2})^{1/3}$ can be rewritten as

$H/D \sim (Q^{*3})^{1/3} = (Q^*)$.

These relationships strongly suggest that the non-dimensional flame height for a fire whirl will be proportional to the non-dimensional heat release rate (Q^*), as indicated by the dotted line in Fig. 8.

Figure 8 shows the correlation between the non-dimensional flame height (H/H_0 or *H/D*) and the non-dimensional heat release rate (Q^*) based on data obtained from these tests. The straight lines in the graph indicate predictions from previous models for a typical pool fire as reported by Cox and Chitty [18], Zukoski [19] and Thomas [20]. The present study covered the range of $1 < Q^* < 10$. In the case of trials without guide plates and with clockwise rotation, the flame height (designated "free" in Fig. 8) agrees with both Zukoski's and Thomas's models. When rotating anticlockwise (for $Q^* = 3$ or greater), the dimensionless flame height, *H/D*, is extended with increases in Q^* and a slender, whirling flame is obtained, with the relationship $H/D = 1.5Q^*$. In the case of a tubular fire whirl, the results fall on the same line as the data for a pool fire model, even though the flame shape is quite different.

Temperature vertical profile along the center axis

To compare the flame behaviour between usual buoyant flames and flames with whirling, as shown in Fig. 9, the relationships between the excess temperature, ΔT, along the central axis of the flame and the height (z) normalized by $Q^{2/5}$ in the flame region was illustrated. This graph includes the line based on the McCaffrey [21] model for the three regions consisting of the flame, intermittent flame and plume. There are evidently different temperature attenuation modes along the central axis of the flame. Figure 9(a) plots the excess temperature profiles along the center axis without guide plates. These values are lower than those for the McCaffrey model, although the attenuation modes were similar to those for McCaffrey's model for a general pool fire. Increasing the rotation tended to increase the excess temperature such that, at a rate of +150 rpm, the flame height had increased to 1.5 times its original value. Because the flame exhibited precession, the flame tip did not remain along the central axis of the flame, and the range of movement of the precessional motion of the flame increased with decreases in the rotation rate. In contrast to a pool fire (as shown in Fig. 9(b)), the rotational flow in a fire whirl with guide plates resulted in active circulation, such that ambient air could not enter into the core part of the lower flame region. Rather, the air gradually entered and combined with the fuel to produce a higher temperature than that in a pool fire. At the same time, the intermittent flame mode disappeared. At rates from +30 to +60 rpm, the flame height was essentially the same as that without guide plates, and the excess temperature attenuation modes were largely the same as McCaffrey's model. This result was obtained because the induced flow was blocked by the accompanied flow, with an effect on the whirling movement of the flame. Comparing the heat release rates and flame heights at +60 rpm with guide plates to those at 57.2 rpm without guide plates shows that the values were very similar. However, the excess temperatures obtained with guide plates were higher than those without plates because the plates eliminated the precessional movement of the flame. The excess temperature range from 800 to 900 °C is associated with the continuous flame region in the McCaffrey model, and $z/Q^{2/5} = 0.08$ is the boundary at which the intermittent flame region begins. In the case of a flame produced with rotation and guide plates, the excess temperature along the flame axis did not show an intermittent region, except at low rotation rates in the range of +30 to +60 rpm. In the region where the $z/Q^{2/5}$ value exceeded 0.2, equivalent to the plume in the McCaffrey model, the excess temperatures obtained with 0 to -90 rpm rotation were higher than those estimated by the model, although a clear intermittent region was not evident.

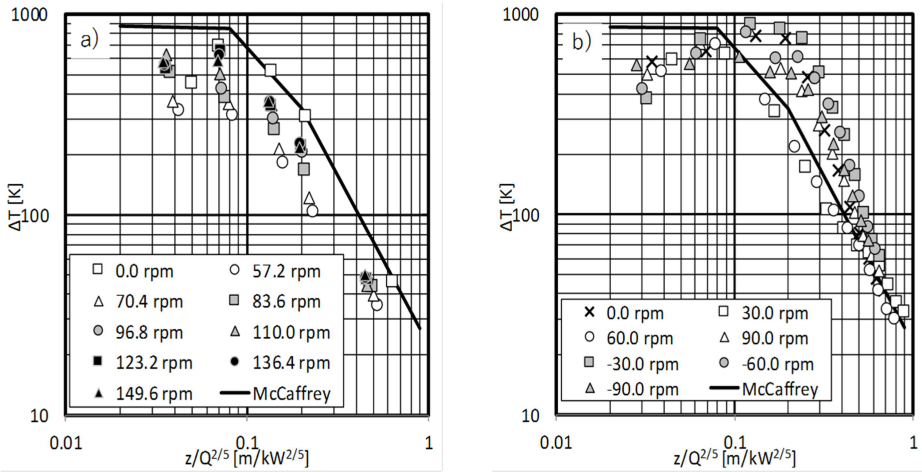

Fig. 9. Temperature attenuation along the central axis of the flame:
a) without guide plates and with rotation and b) with guide plates and with rotation.

Once the attenuation of the excess temperature along the center axis began, the temperature exhibited a greater rate of decrease relative to distance compared with that predicted by the McCaffrey model. These results are attributed to a decrease in the intermittent flame region due to the appearance of a rotating, continuous flame that extended upward. This extension of the continuous flame region was clearly observed in the flame shape. At a $z/Q^{2/5}$ value of 0.6 or larger, representing the plume region, the experimental results were largely the same as those predicted by McCaffrey's model. This excess temperature behaviour indicates that even a fire whirl is simply a diffusion flame system, albeit without an intermittent region.

CONCLUSIONS

These experiments examined flames with and without guide plates and with clockwise or anticlockwise rotation. The following conclusions can be stated.

1) Increases in the rotation rate without guide plates increased the flame height except in the case of slow rotation, during which the flame showed precessional movement.

2) With guide plates, the heat release rate increased with increasing rotation over the range from 0 to -90 rpm. However, the flame height remained steady from -30 to -90 rpm, while the width of the flame increased showing a tubular flame structure after the transition from slender to tubular flame shape. This tubular fire whirl was very similar to those observed by Lei et al. [7] and to a historical painting based on an actual fire whirl that occurred in the aftermath of the earthquake in Tokyo, 1923. This artificial tubular fire whirl was generated using a rotating tube with tilted guide plates.

3) The excess temperature, ΔT, along the center axis of the flame with guide plates showed no or scarcely intermittent flame region, as is observed in a free burning pool fire. The continuous flame region extended upward then transitioned to a plume without forming an intermittent flame region. This behaviour was quite different from that predicted by McCaffrey's model.

ACKNOWLEDGMENTS

The authors sincerely thank Messrs. Kazuki Mihara and Ikuma Okazawa of Sugawa Laboratory, Tokyo University of Science, Suwa, Japan, for their assistance in conducting the tests.

REFERENCES

[1] http://www.youtube.com/watch?v=wQj-5KEqDlg (accessed 28 September 2018).

[2] Collection on https://nekonezumi.exblog.jp/21910775 (accessed 28 September 2018).

[3] S. Soma, Fire Tornado Caused by the Great Fire (Study on the Outbreak Cause of a Fire Tornado at the site of the Former Army Closlenderg Depot), Report of the National Research Institute for Earth Science and Disaster Prevention, 31 (1973) 39-56 (in Japanese).

[4] J.G. Quintiere, Principles of Fire Behavior, Delmar Publishers, Ver. 1 (1998) 3-4.

[5] Y. Mitsuta and N. Monji, Fire-induced Vortices, Disaster Prevention Research Institute Annuals B, 25, B-1 (1982) 255-270 (in Japanese).

[6] A.Yu. Snegirev, J.A. Marsden, J. Francis, G.M. Makhviladze, Numerical studies and experimental observations of whirling flames, Int. J. Heat Mass Transf. 47 (2004) 2523-2539.

[7] J. Lei, N. Liu, Y. Jiao, S. Zhang, Experimental investigation on flame patterns of buoyant diffusion flame in a large range of imposed circulation, Proc. Combust. Inst. 36 (2017) 3149-3156.

[8] S. Ishizuka, Tubular Combustion, Momentum Press, 2013.

[9] A.K. Gupta, D.G. Liley, N. Syred, Swirl Flows, Abacus Press, 1984.

[10] H.W. Emmons, S. Ying, The Fire Whirl, Proc. Combust. Inst. 11 (1967) 475-488.

[11] R. Dobashi, T. Okura, R. Nagaoka, Y. Hayashi, T. Mogi, Experimental Study on Flame Height and Radiant Heat of Fire Whirls, Fire Technol. 52 (2016) 1069-1080.

[12] K.A. Hartl, A.J. Smits, Scaling of a Small Scale Burner Fire Whirl, Combust. Flame 163 (2016) 202-208.

[13] K. Kuwana, S. Morishita, R. Dobashi, K.H. Chuah, K. Saito, The Burning Rate's Effect on the Flame Length of Weak Fire Whirls, Proc. Combust. Inst. 33 (2011) 2425-2432.

[14] J. Lei, N. Liu, J.S. Lozano, L. Zhang, Z. Deng, K. Satoh, Experimental Research on Flame Revolution and Precession of Fire Whirls, Proc. Combust. Inst. 34 (2013) 2607-2615.

[15] J. Lei, N. Liu, Flame Precession of Fire Whirls: A Further Experimental Study, Fire Saf. J. 79 (2016) 1-9.

[16] H. Yua, S. Guoa, M. Penga, Q. Lia, J. Ruanb, W. Wana, C. Chena, Study on the Influence of Air-inlet Width on Fire Whirls Combustion Characteristics, 9th AOSFST, Procedia Eng. 62 (2013) 813-820.

[17] P. Wang, N. Liu, L. Zhang, Y. Bai, K. Satoh, Fire Whirl Experimental Facility with no Enclosure of Solid Walls: Design and Validation, Fire Technol. 51 (2015) 951-969.

[18] G. Cox, R. Chitty, Some Source-Dependent Effects of Unbounded Fires, Combust. Flame 60 (1984) 219-232.

[19] E. Zukoski, Fluid Dynamic Aspects of Room Fire, Proc. of 1st IAFSS (1984) 1-32.

[20] P.H. Thomas, The Size of Flames from Natural Fires, Proc. Combust. Inst. 9 (1963) 844-859.

[21] J.G. McCaffrey, Purely Buoyant Diffusion Flames: Some Experimental Results, NBSIR79-1910, National Bureaus of Standard, Washington, DC, 1979.